

# Medium and Large *N*-Heterocycle Formation via Allene Hydroamination with a Bimetallic Rh(I) Catalyst

Kelton G. Forson, Benjamin O. Bohman, Coriantumr Z. Wayment, Rachel N. Owens, Caitlyn E. McKnight, Rhen C. Davis, Lillian R. Stillwell, Stacey J. Smith, David J. Michaelis\*

Department of Chemistry and Biochemistry, Brigham Young University, Provo, UT 84602.

**KEYWORDS** Catalysis, hydroamination, allene, bimetallic catalysis

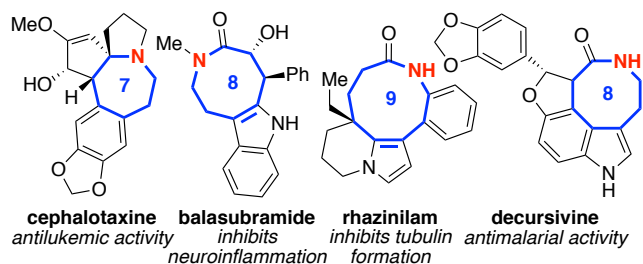
**ABSTRACT:** We report the synthesis of a 2-phosphinoimidazole-derived bimetallic Rh(I) complex containing a bridging CO ligand that facilitates Rh–Rh bond formation. This bimetallic complex enables intramolecular allene hydroamination to form seven to ten-member rings in high yield. Monometallic Rh complexes, in contrast, fail to achieve any product formation. We demonstrate a broad substrate scope for formation of various *N*-heterocycles in good to excellent yields. Macrocyclization reactions that form eleven to fifteen-membered *N*-heterocycles are also demonstrated. Mechanistic studies show that the reaction likely proceeds via catalyst protonation by trifluoroacetic acid, followed by reversible allene insertion into the Rh–H bond and C–N bond-forming reductive elimination. We hypothesize that the difference in product selectivity observed with our catalyst vs monometallic Rh complexes is dependent on the bimetallic nature of our complex.

Nitrogen-containing heterocycles are among the most prevalent structural features in bioactive compounds and pharmaceuticals, and transition metal-catalyzed C–N bond forming reactions represent one of the most efficient and attractive methods for their synthesis.<sup>1</sup> Aminations of metal-allyl intermediates (allylic aminations),<sup>2</sup> oxidative aminations of alkenes,<sup>3</sup> C–H aminations,<sup>4</sup> and alkene or allene hydroaminations<sup>5</sup> represent some of the most widely used methods for metal-catalyzed nitrogen heterocycle synthesis. In general, metal-catalyzed cyclization reactions that proceed via C–N bond formation are highly efficient for 5- and 6-member ring formation, but examples of medium ring formation (7–11 member rings) through these same mechanisms are quite rare.<sup>6</sup> This difficulty of medium-sized ring formation arises because cyclization is inhibited by transannular interactions and bond/torsional strains. This creates a unique challenge in synthesis because many important pharmaceuticals and bioactive natural products contain medium-sized ring nitrogen heterocycles. Figure 1a shows several important examples of bioactive heterocycles in this class. With current technologies, access to medium-sized rings often involves multistep processes and/or ring expansion mechanisms<sup>6c</sup>.

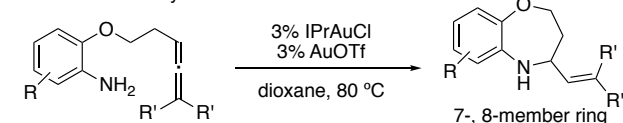
The hydroamination of allenes is an attractive method for nitrogen heterocycle formation as the allene functional group is readily accessible from alkynes and reacts more rapidly than the corresponding alkene substrates.<sup>7</sup> The product of such allene hydroaminations also contains a pendant alkene that is useful for further synthetic manipulations. While Ag, Au, Rh, and Pd are among the most effective catalysts for allene hydroaminations,<sup>7,8</sup> the vast majority of methods only report the formation of 5-, and 6-member rings. In a rare example of medium ring formation via allene hydroamination, Hashmi and coworkers recently reported an Au-catalyzed hydroamination for 7-member ring formation with benzo-fused aniline substrates (Figure

1b).<sup>9</sup> Buchwald also reported an alkene hydroamination under copper catalysis that can generate 7–9-member ring heterocycles from hydroxylamine derivatives (Figure 1c).<sup>10</sup>

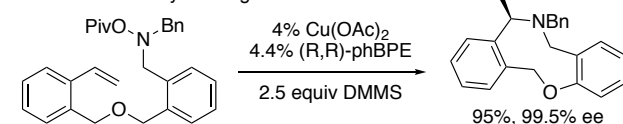
a. Importance of medium-sized ring nitrogen heterocycles



b. Previous work by Hashmi



c. Previous work by Hartwig



d. This work: Bimetallic Rh catalysis form medium-sized rings

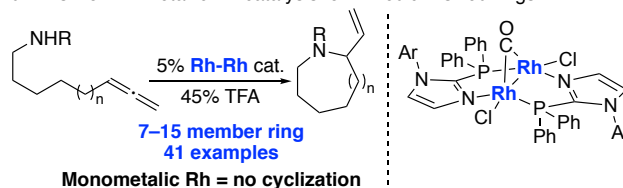


**Figure 1.** Important medium-sized ring heterocycles and methods for their preparation.

Our laboratory is particularly interested in the unique and expanded reactivity that can be accessed via catalysis with hetero- and homobimetallic transition metal complexes. The enhanced bimetallic reactivity possible with these catalysts can result from reactions at metal–metal bonds, sharing electron density through a metal–metal bond, activation of substrates across both metals, or accessing uncommon metal oxidation states in catalysis.<sup>11</sup> Here we report the synthesis of a bimetallic Rh(I) complex scaffolded on 2-phosphinoimidazole ligands (Figure 1c). The formation of this rare example of a bimetallic Rh(I) complex containing a metal–metal bond is facilitated by a bridging CO ligand. Our new complex is also catalytically active in intramolecular allene hydroamination reactions and uniquely enables the formation of medium-sized rings (7–11 member rings) and macrocyclic rings (12–15 member rings). Importantly, monometallic Rh catalysts fail to achieve cyclization and heterocycle formation for medium sized rings. Our bimetallic rhodium complex enables efficient hydroaminations with a variety of amine nucleophiles and for formation of numerous heterocyclic core structures. Mechanistic studies also confirm the role of the rhodium catalyst in product formation.

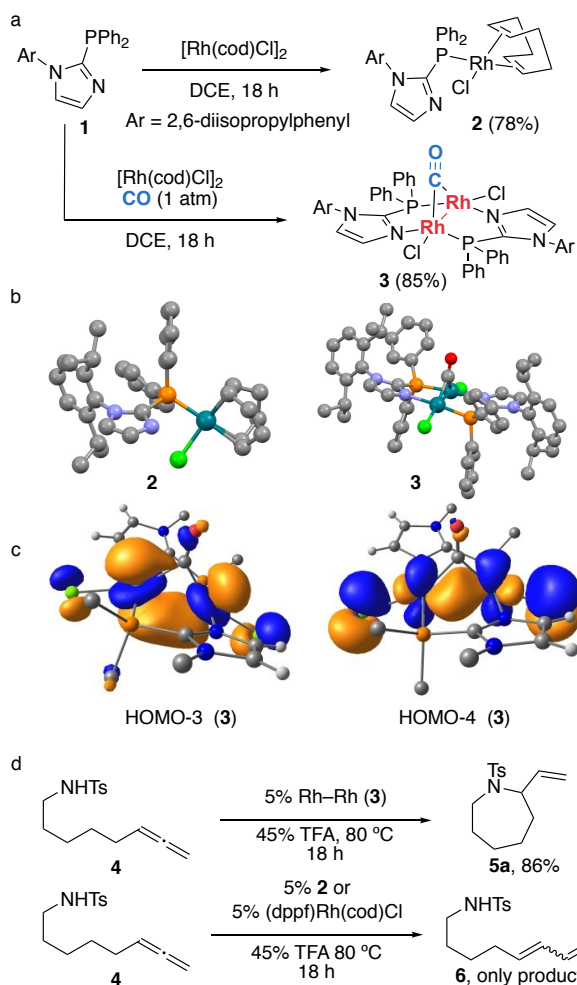


**Figure 2.** a) Synthesis of mono and bimetallic Rh phosphinoimidazole complexes. b) X-ray crystal structures of **1** and **2**. c) Selected Kohn–Sham orbitals (BP86/6-311G(d,p)) for the computationally optimized structure of **3** (*P*-aryl and *N*-aryl substituents of **3** were removed for clarity). d) Reactivity of monometallic and bimetallic Rh complexes with allene substrates.

We recently reported the synthesis of 2-phosphinoimidazole-derived bimetallic Pd(I) and Pd(II) complexes and their exceptional reactivity in a tandem ketone  $\alpha$ -arylation annulation reactions for naphthalene synthesis.<sup>12</sup> In an attempt to expand the applications of these ligands to bimetallic catalysis, we attempted the synthesis of the corresponding Rh complexes. When 2-phosphinoimidazole ligand **1** was reacted with  $[\text{Rh}(\text{cod})\text{Cl}]_2$ , monometallic complex **2** was formed (Figure 2a). The crystal structure of **2** shows only phosphine binding, which suggests that coordination of both the P and the N of the 2-phosphinoimidazole is unfavorable due to a non-ideal bite angle (Figure 2b). When the reaction of **1** with  $[\text{Rh}(\text{cod})\text{Cl}]_2$  was run in methanol, however, a trace amount of bimetallic complex **3** was observed, presumably via methanol oxidation. When the same reaction was performed in DCE solvent and under an atmosphere of CO, bimetallic complex **3** could be isolated in excellent yield (85% yield). No bimetallic complex is observed in the absence of a CO ligand under the same conditions.

The X-ray crystal structure of **3** shows the presence of a bridging CO ligand, which we believe necessary for formation of the bimetallic complex. We believe that coordination of a bridging CO ligand allows the two rhodium centers to achieve a suitable distance on the ligand framework to form a stable complex. The Rh–Rh bond distance for complex **3** is 2.6227 Å, and the formal shortness ration (FSR) of the Rh–Rh bond is 1.05.<sup>13</sup> These data suggest that the metals are in close enough proximity to form a Rh–Rh bond, wherein the CO ligand would serve as a “ketone-like” ligand and not form a 2-electron, 3-center bond.<sup>14</sup> This would suggest that the CO ligand facilitates formation of high-spin Rh centers, which enables M–M bond

**Table 1.** Optimization of hydroamination reaction.

entry <sup>a</sup>	mol% cat.	temp.	mol% acid	yield <sup>b</sup>
1	5	80 °C	0	0%
2	5	80 °C	15	16%
3	5	80 °C	30	61%
4	5	80 °C	45	90%
5	5	50 °C	45	62%
6	5	23 °C	45	24%
7 <sup>c</sup>	5	80 °C	45	83%
8	2.5	80 °C	45	57%
9	1	80 °C	45	15%
10	5	80 °C	45 (TfOH)	0%
11	5	80 °C	45 (TsOH)	0%
12	5	80 °C	45 (AcOH)	0%
13	0	80 °C	45	0%

<sup>a</sup> Reaction run on a 0.2 mmol scale of **4** with 5 mol% Rh dimer **3** and 45% TFA in dichloroethane (DCE, 0.2 M) at 80 °C for 18 h unless otherwise noted. <sup>b</sup> Conversions determined by <sup>1</sup>H NMR analysis of the crude reaction mixture by comparing product peaks with remaining starting material. <sup>c</sup> Reaction run in toluene.

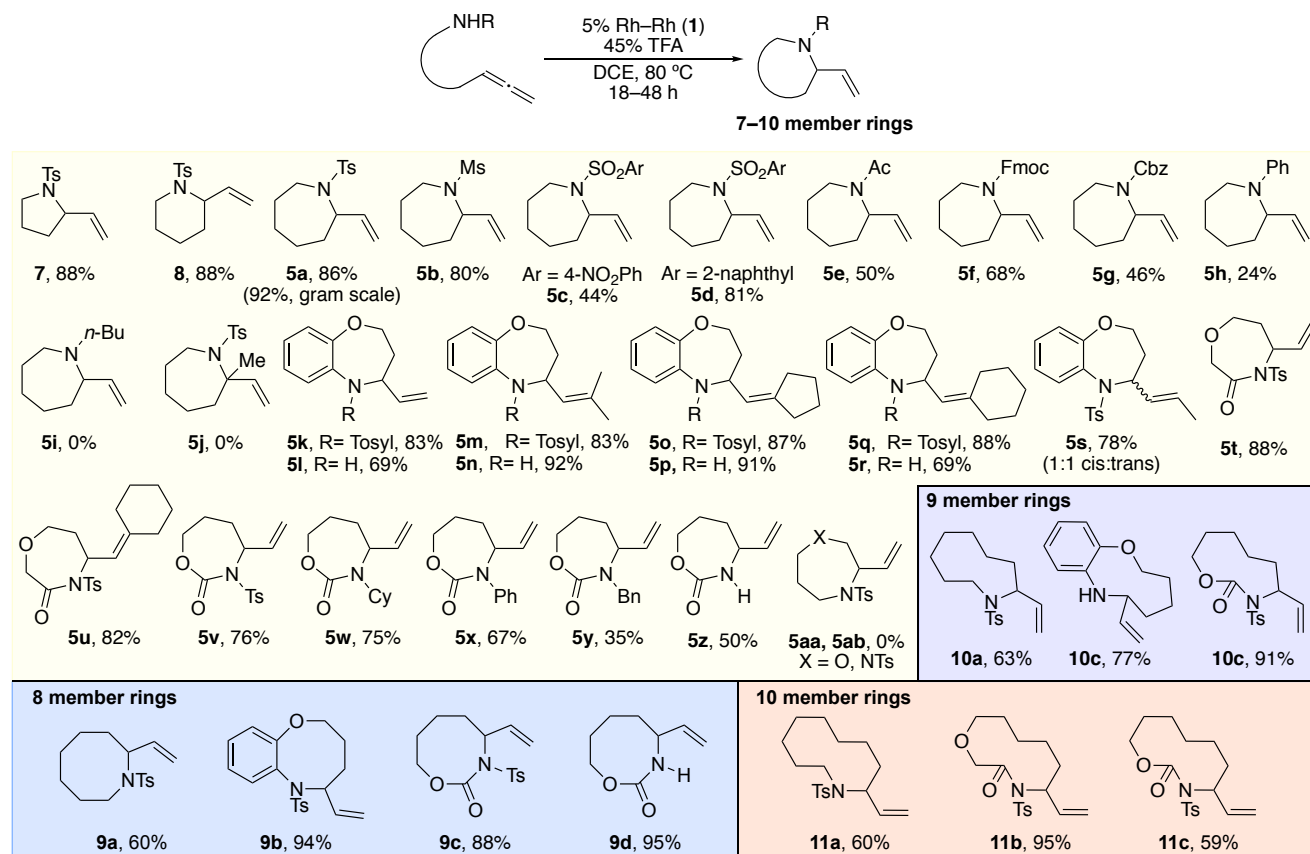


**Figure 3.** Substrate scope for 7–10-member ring formation via allene hydroamination catalysis. Conditions:

formation by creating unpaired electrons at each metal. DFT computed Kohn-Sham orbitals also support the formation of a metal-metal bond (Figure 2c). The HOMO-3 and HOMO-4 orbitals of **3** show shared electron density between the two metals, supporting our hypothesis that complex **3** contains a metal-metal bonding interaction.

Our new bimetallic Rh complex is a rare example of a homobimetallic Rh(I) complex containing a metal-metal bond. Catalytic applications of dirhodium complexes have centered around the use of Rh(II) tetracarboxylates and carboxamides.<sup>15</sup> Examples of catalysis with intact bimetallic Rh(I) complexes where the two metals form a bond are very rare.<sup>16</sup> Thus, we sought to investigate the potential of this complex to enable reactivity not accessible with monometallic catalysts. Rh(I) catalysts traditionally have high reactivity in allene hydroamination reactions, and we found that complex **3** enables rapid hydroaminations of allenes to form 5- and 6-membered rings (see Figure 3). Since our catalyst displays an expanded coordination sphere that includes two rhodium centers, we wondered whether catalyst **3** could enable medium ring formation by altering the geometry of the C–N bond forming event. When substrate **4** was subjected to hydroamination with complex **3**, the corresponding seven-member ring was isolated in excellent yield (Figure 2d). Rhodium-catalyzed hydroaminations of this class of linear allenes for medium-sized ring formation have not been previously reported. Importantly, when we used either monometallic complex **2** or dppf + [Rh(cod)Cl]<sub>2</sub>, only the isomerized diene product **6** was observed, and no heterocycle formation occurred. This diene product is presumably formed via  $\beta$ -hydride elimination from a metal allyl intermediate instead of C–N bond forming reductive elimination that occurs with **3**.

Being intrigued by the unique ability of **3** to enable 7-member ring formation, we next set out to verify the importance of the reaction conditions to catalysis (Table 1). We found that trifluoroacetic acid (TFA) was essential for the reaction and that higher loadings of acid led to faster catalysis (Entries 1–4). We also found that higher temperatures were required for good conversion (entries 4–6), and that the reaction could also be run in toluene (entry 7). Lower catalyst loadings also led to lower conversions (entries 7–9). When either stronger acid (triflic acid (TfOH) or *p*-toluenesulfonic acid (TsOH), entries 10–11) or weaker acid (acetic acid (AcOH), entry 12) were employed, lower yields were obtained. No product formation was observed in the absence of the rhodium catalyst (entry 13).

With optimized conditions, we next investigated the types of heterocycles and ring sizes that could be accessed with our new catalyst (Figure 3). Both five (**7**) and six-membered rings (**8**) are efficiently formed with our catalyst. For seven-membered rings, substrates containing various groups on the nitrogen nucleophile reacted in good yield, including various substituted sulfonamides (**5a–5d**), acetamides (**5e**), carbamates (**5f**, **5g**), and anilines (**5h**). *N*-alkylamines (**5i**), however, failed to give any product formation, presumably due to reaction of the amine with the strong acid in the mixture. We also found that sterically hindered 3,3-disubstituted allenes failed in the reaction (**5j**) under our standard conditions. Similar to work by Hashmi, we found that various arene-bridged substrates containing 1,1-disubstituted allenes also reacted in high yield to give the 7-member ring products (**5k–5s**).<sup>9</sup> Unlike previous studies, our catalyst efficiently cyclizes amine substrates that contain monosubstituted allenes (**5k**, **5l**) and electron-withdrawing sulfonyl groups on the aniline derivative (**5k**, **5m**, **5o**, **5q**, **5s**). With 1,3-

disubstituted allenes, we isolated the product as a 1:1 mixture of alkene isomers (**5s**). A variety of other 7-membered heterocycles can also be formed via our method, including ether-containing lactams (**5t**, **5u**) and cyclic carbamates (**5v–5z**). Substrates with heteroatoms at the allylic position failed to give any reaction with our catalyst (**5aa**, **5ab**), likely due to deactivation of the allene by the proximal electron withdrawing group. We also found that our reaction is easily scalable; when the reaction was conducted on gram scale (3.6 mmol), 92% yield of product **5a** was obtained.

We next sought to investigate the different sizes of medium-sized rings that could be formed via our cyclization reaction (Figure 3). For 8-member ring formation, aliphatic *N*-sulfonyl heterocycles (**9a**), arene-bridged substrates (**9b**), and carbamates (**9c**, **9d**) all reacted in good to excellent yield. As with 7-member ring formation, no cyclized product is observed when a monometallic Rh catalyst (dppf + [RhcodCl]<sub>2</sub>) is employed in the reaction with **9a**. Both 9-member and 10-member substrates also cyclize with our catalyst to provide the products in good yield. For example, sulfonamide (**10a**, **11a**), *N*-tosyl amide (**11b**), aniline derivatives (**10c**), and carbamates (**10c**, **11c**), all reacted in high yield to give the corresponding cyclized nine and ten-membered products.

We also wanted to see if we could expand the ring-forming hydroamination to include larger heterocycles via macrocyclization (Figure 4). With our catalyst bimetallic **3**, large ring heterocycles from 11-member to 15-member rings (**12a–12e**) were readily formed in high yield. In contrast to reports by Hashmi for 7-member ring formation,<sup>9</sup> we did not observe detectable amounts of dimer or oligomer products in any of our cyclization reactions. These results represent a rare example of macrocyclization via a hydroamination mechanism and highlight the synthetic utility of our bimetallic catalyst.<sup>10,17</sup>

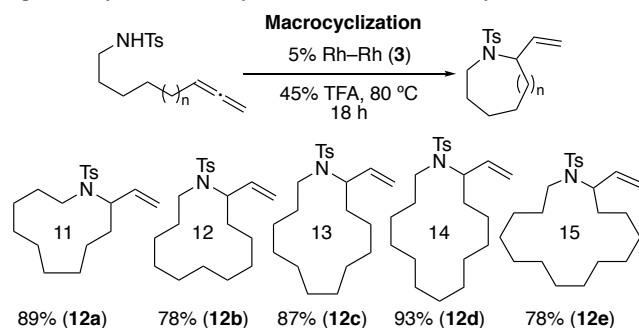


**Figure 4.** Macrocyclization via hydroamination with **3**.

To investigate the mechanism of the hydroamination with our bimetallic Rh catalyst, we first performed the reaction with deuterated substrate **4a-D** with deuterio-TFA (Figure 5a). Consistent with previous studies by Breit,<sup>8d</sup> we found deuterium incorporation at all carbons of the allene. This suggests that the mechanism likely proceeds via initial oxidative addition of the Rh to trifluoroacetic acid to generate a Rh hydride. This hydride then undergoes reversible insertion into the alkene to generate a metal allyl intermediate, followed by a final product-forming reductive elimination via C–N bond formation. Interestingly, we observed a small amount of diene **6** in the crude reaction mixture with catalyst **3** and substrate **5a**. This led us to wonder whether diene **6** could be converted to the heterocycle product via hydroamination of the diene and formation of a Rh-allyl intermediate. A significant amount of deuterium incorporation at the position beta to the nitrogen in the heterocycle product (13%) suggests that reversible formation of the diene does

happen in the reaction prior to C–N bond-forming reductive elimination (see Figure 5a). This result confirms that while diene **6** is formed in the presence of our bimetallic catalyst, it can be converted to the desired heterocyclic product.

A proposed catalytic cycle based on these observations is shown in Figure 5b. Initial oxidative addition of bimetallic complex **3** into the O–H bond of TFA can generate either **A** or **B**, depending on whether oxidative addition occurs across one or both metals. Subsequent reversible Rh-hydride insertion into the allene and coordination of the amine nucleophile with loss of TFA then provides intermediate **C**. Intermediate **C** could have the nitrogen nucleophile bound to either of the two rhodium centers prior to reductive elimination. While **C** could undergo beta-hydride elimination to form diene intermediate **D**, our studies suggest that this process is reversible. Reductive elimination and C–N bond formation gives intermediate **E**, and loss of product then provides the cyclized product and regenerates **3**.

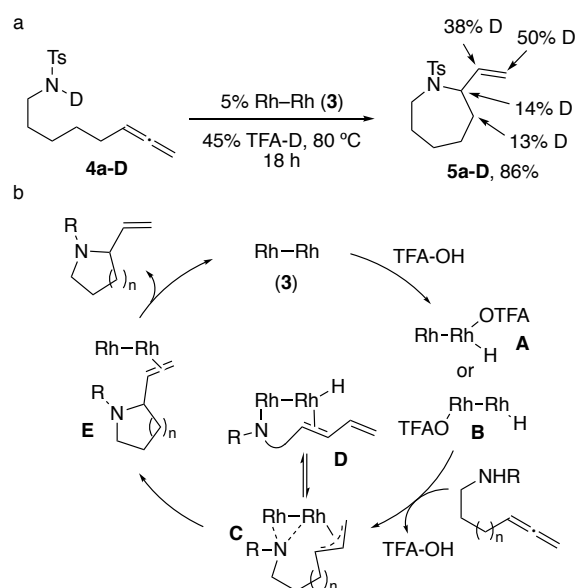


**Figure 5.** Mechanistic studies and proposed mechanism.

We hypothesize that the bimetallic structure of **3** may be the key factor in enabling cyclization and heterocycle formation when monometallic catalysts fail. This could result from electronic communication between the two metal centers that lowers the barrier for reductive elimination and accelerates heterocycle formation.<sup>11</sup> Alternatively, coordination of the two reacting partners, the metal allyl and the nitrogen nucleophile, to the two metal centers could bring the partners into close proximity and facilitate ring formation. The expanded size of a cyclic intermediate containing two rhodium atoms could also help alleviate transannular strain interactions that inhibit medium-sized ring formation. Current DFT studies in our laboratory are exploring these and other possible mechanisms to understand how the bimetallic complex changes reactivity in this system.<sup>12a, 18</sup> These results will be communicated in due time.

In conclusion, we have discovered a bimetallic dirhodium(I) complex that is catalytically active in allene hydroamination reactions. Our catalyst is uniquely able to cyclize medium-sized ring substrates where monometallic Rh catalysts failed, providing easy synthetic access to a variety of 8–10-membered ring heterocycles. Our bimetallic catalyst also enables macrocyclization reactions to efficiently form 11–15-member ring

heterocycles. Mechanistic experiments confirm the importance of the bimetallic catalyst and acid in catalysis, suggesting a metal-hydride insertion mechanism that is followed by C–N bond forming reductive elimination. Our ongoing mechanistic studies are focused on understanding how the bimetallic nature of the catalyst enables highly efficient medium-sized ring formation and macrocyclization.

## ASSOCIATED CONTENT

### Supporting Information

The Supporting Information is available free of charge on the ACS Publications website.

Experimental procedures and spectral information for new compounds (PDF)

X-ray crystallographic information (CIF)

## AUTHOR INFORMATION

### Corresponding Author

dmichaelis@chem.byu.edu

## ACKNOWLEDGMENT

We thank the United States National Science Foundation Synthesis Program for partial support of this work (CHE 1665015).

## REFERENCES

1. a) Catalyzed Carbon-Heteroatom Bond Formation. Yudin, A. K., Ed. Wiley-VHC, 2011, Weinheim, Germany. b) Majumdar, K. C.; Debnath, P.; De, N. Roy, B. Metal-catalyzed Heterocyclization: Synthesis of five- and six-membered Nitrogen Heterocycles Through Carbon-Nitrogen Bond Forming Reactions. *Curr. Org. Chem.* **2011**, *15*, 1760–1781.
2. Grange, R. L.; Clizbe, E. A.; Evans, P. A. Recent Developments in Asymmetric Allylic Amination Reactions. *Synthesis* **2016**, *48*, 2911–2968.
3. Thomas, A. A.; Nagamalla, S.; Sathyamoorthi, S. Salient features of the aza-Wacker cyclization reaction. *Chem. Sci.* **2020**, *11*, 8073–8088.
4. Kazerouni, A. M.; McKoy, Q. A.; Blakey, S. B. Recent advances in oxidative allylic C–H functionalization via group IX-metal catalysis. *Chem. Rev.* **2020**, *56*, 12287–12300. b) Park, Y.; Kim, Y.; Chang, S. Transition Metal-Catalyzed C–H Amination: Scope, Mechanism, and Applications. *Chem. Rev.* **2017**, *117*, 9247–9301.
5. a) Rocard, L.; Chen, D.; Stadler, A.; Zhang, H.; Gil, R.; Bezenine, S.; Hannedouche, J. Earth-Abundant 3d Transition Metal Catalysts for Hydroalkoxylation and Hydroamination of Unactivated Alkenes. *Catalysts* **2021**, *11*, 674. b) Wang, H.; Buchwald, S. L. Copper-catalyzed, enantioselective hydrofunctionalization of alkenes. *Org. React.* **2019**, *100*, 121–195. c) Trowbridge, A.; Walton, S. M.; Gaunt, M. J. New Strategies for the Transition-Metal Catalyzed Synthesis of Aliphatic Amines. *Chem. Rev.* **2020**, *120*, 2613–2692. d) Beccalli, E. M.; Broggin, G.; Christodoulou, M. S.; Giofrè, S. Transition metal-catalyzed intramolecular amination and hydroamination reactions of allenes. *Adv. Organometal. Chem.* **2018**, *69*, 1–71. e) Reznichenko, A. L.; Hultsch, K. C. Hydroamination of alkenes. *Org. React.* **2016**, *88*, 1–554. f) Huang, L.; Arndt, M.; Gooßen, K.; Heydt, H.; Gooßen, L. J. Late Transition Metal-Catalyzed Hydroamination and Hydroamidation. *Chem. Rev.* **2015**, *115*, 2596–2697.
6. a) Reyes, R. L.; Iwai, T.; Sawamura, M. Construction of Medium-Sized Rings by Gold Catalysis. *Chem. Rev.* **2021**, *121*, 8926–8947. b) Choury, M.; Basilio Lopes, A.; Blond, G.; Gulea, M. Synthesis of Medium-Sized Heterocycles by Transition-Metal-Catalyzed Intramolecular Cyclization. *Molecules* **2020**, *25*, 3147. c) Yet, L. Metal-Mediated Synthesis of Medium-Sized Rings. *Chem. Rev.* **2000**, *100*, 2963–3008. c) Clarke, A. K.; Unsworth, W. P. A happy medium: the synthesis of medicinally important medium-sized rings via ring expansion. *Chem. Sci.* **2020**, *11*, 2876–2881. d) Nubbemeyer, U. Synthesis of Medium-Sized Ring Lactams. *Top. Curr. Chem.* Vol. 216, Springer-Verlag, Berlin, Heidelberg, 2001.
7. Beccalli, E. M.; Broggin, G.; Christodoulou, M. S.; Giofrè, S. Transition Metal-Catalyzed Intramolecular Amination and Hydroamination Reactions of Allenes. In *Advances in Organometallic Chemistry*, vol 69 (2018), Elsevier inc.
8. For leading references, see: a) Meguro, M.; Yamamoto, Y. A new method for the synthesis of nitrogen heterocycles via palladium catalyzed intramolecular hydroamination of allenes. *Tetrahedron Lett.* **1998**, *39*, 5421–5424. b) Hamilton, G. L.; Kang, E. J.; Mba, M.; Toste, F. D. A Powerful Chiral Counterion Strategy for Asymmetric Transition Metal Catalysis. *Science* **2007**, *317*, 496–499. c) Zhang, Z.; Bender, C. F.; Widenhoefer, R. A. Gold(I)-Catalyzed Dynamic Kinetic Enantioselective Intramolecular Hydroamination of Allenes. *J. Am. Chem. Soc.* **2007**, *129*, 14148–14149; d) Berthold, D.; Geissler, A. G. A.; Giofrè, S.; Breit, B. Rhodium-Catalyzed Asymmetric Intramolecular Hydroamination of Allenes. *Angew. Chem. Int. Ed.* **2019**, *58*, 9994–9997.
9. a) Pflsterer, D.; Dolbundalchok, P.; Rafique, S.; Rudolph, M.; Rominger, F.; Hashmi, A. S. K. On the Gold-Catalyzed Intramolecular 7-exo-trig Hydroamination of Allenes. *Adv. Synth. Catal.* **2013**, *355*, 1383–1393. b) Yang, W.; K. Hashmi, A. S. K. Mechanistic insights into the gold chemistry of allenes. *Chem. Soc. Rev.* **2014**, *43*, 2941–2955.
10. Dai, X.-J.; Engl, O. D.; León, T.; Buchwald, S. L. Catalytic Asymmetric Synthesis of  $\alpha$ -Arylpyrrolidines and Benzo-fused Nitrogen Heterocycles. *Angew. Chem. Int. Ed.* **2019**, *58*, 3407–3411.
11. a) Farley, C. M.; Uyeda, C. Organic Reactions Enabled by Catalytically Active Metal-Metal bonds. *Trends Chem.* **2019**, *1*, 497–509. b) Powers, I. G.; Uyeda, C. Metal–Metal Bonds in Catalysis. *ACS Catal.* **2017**, *7*, 936–958. c) Pye, D. R.; Mankad, N. P. Bimetallic Catalysis for C–C and C–X Coupling Reactions. *Chem. Sci.* **2017**, *8*, 1705–1718. d) Cooper, B. G.; Napoline, J. W.; Thomas, C. M. Catalytic Applications of Early/Late Heterobimetallic Complexes. *Catal. Rev.* **2012**, *54*, 1–40. (e) Ritleng, V.; Chetcuti, M. J. Hydrocarbyl Ligand Transformations on Heterobimetallic Complexes. *Chem. Rev.* **2007**, *107*, 797–858.
12. a) Ence, C. C.; Martinez, E. E.; Himes, S. R.; Nazari, S. H.; Rodriguez Moreno, M.; Matu, M. F.; Larsen, S. G.; Gassaway, K. J.; Valdivia-Berroeta, G. A.; Smith, S. J.; Ess, D. H.; Michaelis, D. J. Experiment and Theory of Bimetallic Pd-Catalyzed  $\alpha$ -Arylation and Annulation for Naphthalene Synthesis. *ACS Catal.* **2021**, *11*, 10394–10404. b) Martinez, E. E.; Rodriguez Moreno, M.; Barksdale, C. A.; Michaelis, D. J. Effect of Precatalyst Oxidation State in C–N Cross-Couplings with 2-Phosphinoimidazole-Derived Bimetallic Pd(I) and Pd(II) Complexes. *Organometallics* **2021**, *40*, 2763–2767.
13. Chipman, J. A.; Berry, J. F. Paramagnetic Metal–Metal Bonded Heterometallic Complexes. *Chem. Rev.* **2020**, *120*, 2409–2447.
14. Green, J. C.; Green, M. L. H.; Parkin, G. The occurrence and representation of three-centre two-electron bonds in covalent inorganic compounds. *Chem. Commun.* **2012**, *48*, 11481–11503.
15. a) Doyle, M. P. Perspective on dirhodium carboxamidates as catalysts. *J. Org. Chem.* **2006**, *71*, 9253–9250. b) Davies, H. M. L.; Liao, K. Dirhodium tetracarboxylates as catalysts for selective intermolecular C–H functionalization. *Nature Rev. Chem.* **2019**, *3*, 347–360. c) Rhodium Catalysis in Organic

- Synthesis: Methods and Reactions; Tanaka, K. Ed.; Wiley-VCH, 2019.
16. a) Jurt, P.; Salnikov, O. G.; Gianetti, T. L.; Chukanov, N. V.; Baker, M. G.; Le Corre, G.; Borger, J. E.; Verel, R.; Gauthier, S.; Fuhr, O.; Kovtunov, K. V.; Fedorov, A.; Fenske, D.; Kopytyug, I. V.; Grützmacher, H. Low-valent homobimetallic Rh complexes: influence of ligands on the structure and the intramolecular reactivity of Rh–H intermediates. *Chem. Sci.* **2019**, *10*, 7937–7945. b) Weller, A. S.; McIndoe, J. S. Reversible Binding of Dihydrogen in Multimetallic Complexes. *Eur. J. Inorg. Chem.* **2007**, *28*, 4411–4423.
  17. Kranemann, C. L.; Costisella, B.; Eilbracht, P. A new and versatile access to azamacroheterocycles via ring closing carbonylative hydroaminomethylation. *Tetrahedron Lett.* **1999**, *40*, 7773–7776.
  18. Walker, W. K.; Kay, B. M.; Michaelis, S. A.; Anderson, D. L.; Smith, S. J.; Ess, D. H.; Michaelis, D. J. Origin of Fast Catalysis in Allylic Amination Reactions Catalyzed by Pd–Ti Heterobimetallic Complexes. *J. Am. Chem. Soc.* **2015**, *137*, 7371.

